Supplemental Materials

Opposite actions of Angiopoietin-2 on Tie2 signaling and Foxo1 activation in the presence or absence of inflammation (Kim et al.)

Supplemental Methods

REGN910 binding affinity and validation for immunohistochemistry. The affinity of REGN910 for mouse Ang1 was measured in surface plasmon resonance Biacore experiments (1). Briefly, mouse Ang1 fibrinogen domain fused to mouse Fc (produced at Regeneron) was injected at a range of concentrations over a REGN910-captured surface. No binding to mouse Ang1 was observed, in contrast to the positive control human Ang2 fibrinogen domain-mouse Fc, which bound with an affinity of ~10pM. The lack of binding of REGN910 to mouse Ang1 is consistent with the lack of binding to human Ang1 previously reported (1).

Mouse ovary and uterus, known locations of Ang2 expression (2, 3), were examined as validation of REGN910 for localizing Ang2 by immunohistochemistry. Ovary and uterus were removed from 8-week old female mice, embedded in Tissue-Tek medium (Sakura, Torrance, CA), and frozen as cryostat blocks. Ovary and uterus cut into 20-μm thick sections were mounted and stained with REGN910. Also, as further validation, REGN910 immunoreactivity was tested in HUVEC (Lonza, #C2519A) under baseline (control) conditions, with co-staining for vWF, and after stimulation with 50 ng/mL phorbol 12-myristate 13-acetate (PMA) (Sigma-Aldrich, St Louis, MO) for 30 min to induce release of Weibel-Palade bodies containing Ang2 and vWF. Simultaneous loss of REGN910 and vWF immunoreactivities from the same intracellular compartment (Weibel-Palade bodies) was considered consistent with Ang2-labeling by REGN910 (4).

Soluble Tie1 measurement. Soluble Tie1 in mouse serum was measured by ELISA according to the method developed by Korhonen et al (5). In brief, a 96-well plate was coated with human anti-hTie1 antibody (1µg/ml, Dyax) in PBS and incubated at 4^0C. The wells were washed three times with PBS containing 0.1% Tween20, followed by blocking with PBS containing 0.1% Tween20 and 1% bovine serum albumin (BSA) for 1 hour at room temperature. The wells were washed three times with PBS containing 0.1% Tween20. Samples, standards (mTie1-Fc, Reliatech), and blank solution were diluted in 1% BSA in PBS, pipetted into wells (100 µl/well), and incubated for 2 hours at room temperature. The wells were washed three times and then incubated with goat-anti-hTie1 capture antibody (0.5 µg/ml, R&D, AF619) for 1 hour at room temperature. The wells were washed three times, incubated with rabbit-anti-goat-HRP (diluted 1:1000) for 30 min, washed and followed by incubation with substrate solution for 10 min. After adding 1M HCl stop solution, absorbance was measured at 450 nm using a Multiscan Ascent spectrophotometer (Thermo Labsystems).

Mouse genotyping. Mice were genotyped by PCR analysis of genomic tail DNA using the following primers:

Mice	Gene	Forward (5' – 3')	Reverse (5' – 3')
Tie1-Ang2	tTA transgene	CGCTGTGGGGCATTTTACTTTAG	CATGTCCAGATCGAAATCGTC
	tetO-Ang2 transgene	ATCCTGCCTTTCTCTTTATGGTT	AGCCTTTGCACTGAGTCGTCGTA
Ang2-EGFP	Angpt2 (000302) F	GGAAGGAAAGTGATTGATTCGGATAC	--
	GS eGFP R3	--	GGTCGGGGTAGCGGCTGAA
CC10-VEGF-A	rtTA transgene	CCTCGATGGTAGACCCGTAA	CGCAATGGAGCAAAAGTACA

Morphometric measurements. Area density and fluorescence intensity were measured in blood vessels identified by CD31 staining as an index of protein abundance, using ImageJ software (version 1.46, http://imagej.nih.gov/ij/, NIH, Bethesda, MD). Area density was calculated as the percentage of total pixels with fluorescence intensity above a threshold value of 85 to 95 in the range of 0 to 255. Fluorescence intensity of p-Tie2, Tie1 and Tie2 was calculated as the cumulative percentage of pixels between intensities 0 to 255 or as the mean fluorescence intensity. The mean value for each group was calculated from the average of values for each mouse.

Statistical analysis. Supplemental data for cumulative fluorescence intensity are presented as the difference in the cumulative percentage of pixels from control over the intensity range 0 to 255. Cumulative percentage curves were assessed by Kolmogorov-Smirnov 2-Sample Test. Supplemental data for mean fluorescence intensities are presented as mean ± SEM, assessed by 1-way ANOVA followed by the Bonferroni test for multiple comparisons. *P* values less than 0.05 were considered statistically significant (n = 4-9 mice per group).

A

Test Ligand : mAng1 FD-mFC					
mAb Capture (RU)	**30 nM Ag Binding (RU)**	**k_a ($M^{-1}s^{-1}$)**	**k_d (s^{-1})**	**K_D(M)**	**$T_{1/2}$ (min)**
382.7	-1.9	NB	NB	NB	NB

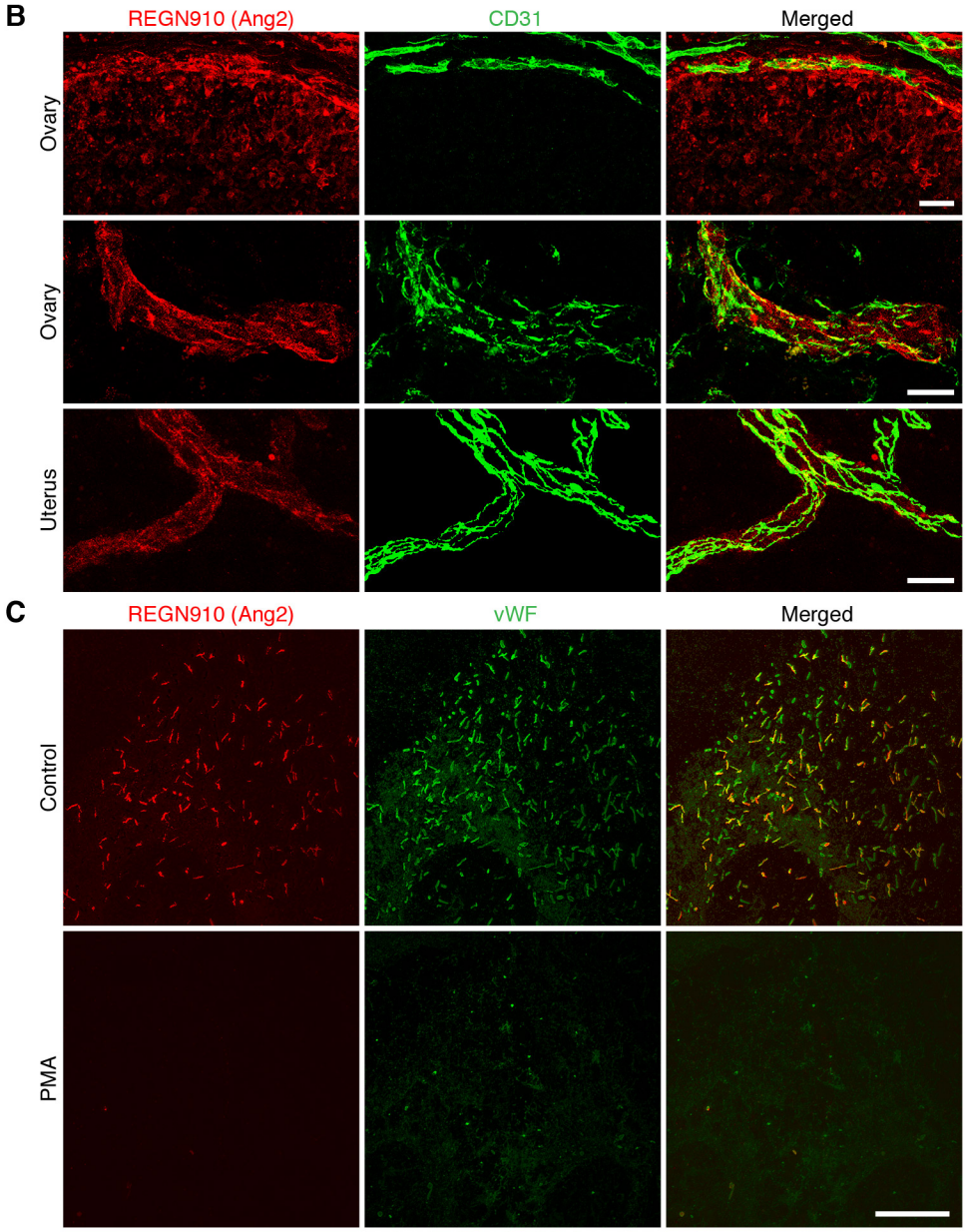

Supplemental Figure 1. Specificity of REGN910 antibody for Ang2. (**A**) Biacore analysis showing no binding (NB) of REGN910 to mouse Ang1. (**B**) Strong REGN910 immunoreactivity near blood vessels in the theca interna of an ovarian follicle (top), a known location of Ang2 expression (3). REGN910 immunoreactivity in some vessels of ovarian cortex (middle) and in endometrial blood vessels of uterus (bottom). (**C**) Structured illumination microscopic image of HUVEC with expression of Ang2 shown by REGN910 immunofluorescence that colocalizes with vWF in rod-shaped Weibel-Palade bodies under baseline conditions (5), but neither is detectable after PMA stimulation. Scale bars in B and C, 10 µm.

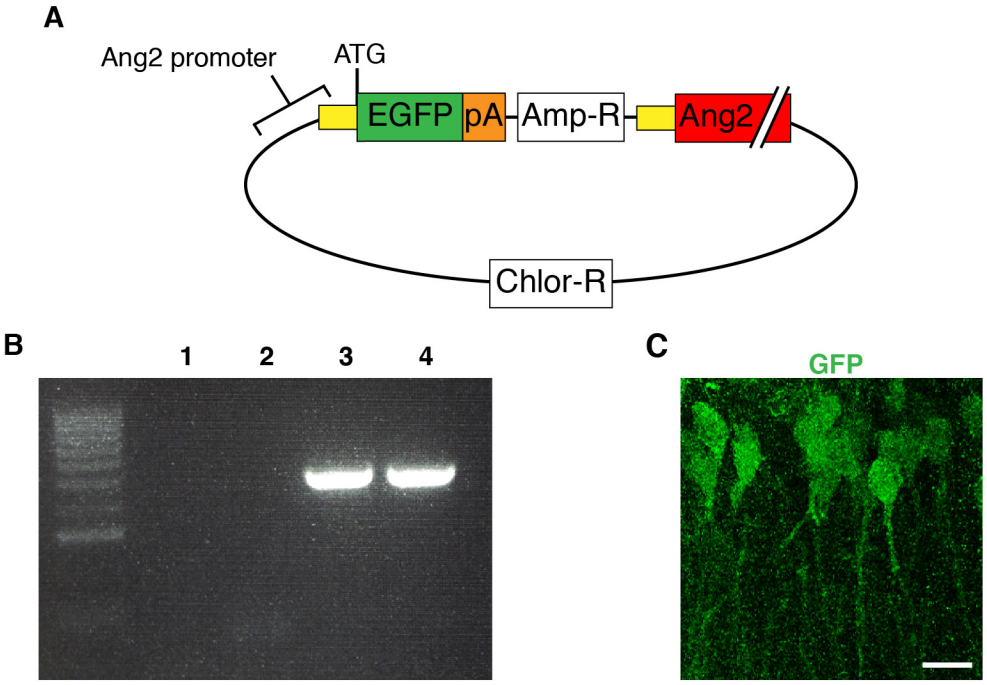

Supplemental Figure 2. Generation of Ang2-EGFP transgenic mice in the GENSAT BAC transgenic project. (**A**) Schematic diagram of *Angpt2* gene targeting with the GFP reporter gene via homologous recombination (diagram modified from (6)). (**B**) PCR-genotyping of Ang2-EGFP transgenic mice comparing non-transgenic negative controls (lanes 1 and 2) and Ang2-EGFP pups (lanes 3 and 4). (**C**) Presence of GFP immunoreactivity in neurons of the hippocampus, a known location of Ang2 in the brain, of Ang2-EGFP mouse at age 8 weeks. Scale bar, 20 µm.

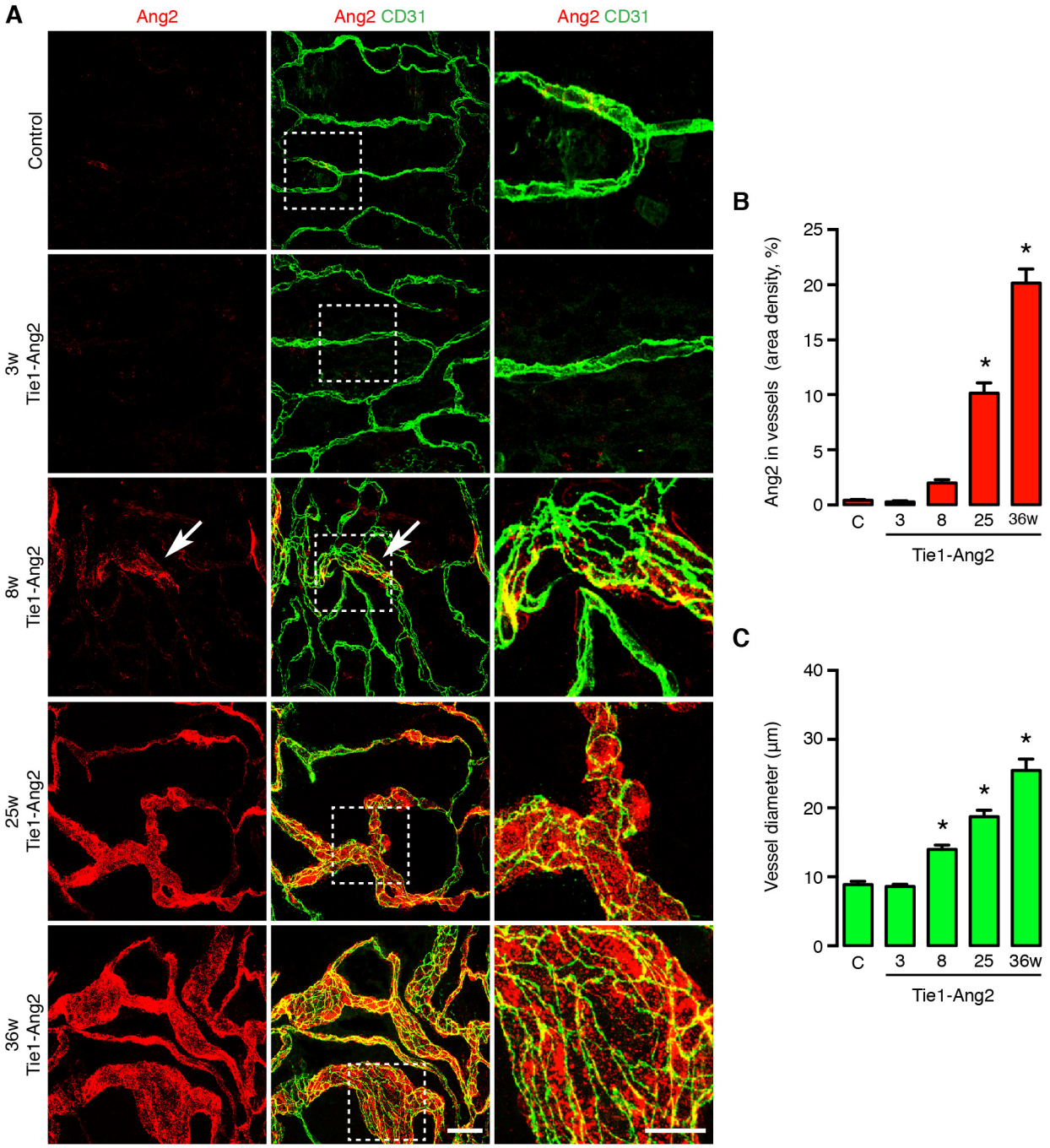

Supplemental Figure 3. Age-related increase in Ang2 and vascular remodeling in Tie1-Ang2 mice. (**A**) Progressive increase in Ang2 immunofluorescence and vascular enlargement in tracheal blood vessels of pathogen-free Tie1-Ang2 mice off doxycycline from birth to age 3, 8, 25, or 36 weeks. Arrows mark enlarged vessels in Tie1-Ang2 mouse at age 8 weeks. Boxed regions are enlarged in right-most column. Scale bar, 50 µm. (**B** and **C**) Measurements of Ang2 staining (**B**) and capillary size (**C**) over cartilage rings of control and Tie1-Ang2 mice, showing age-related increases in both readouts (n = 4-12 per group). *$P < 0.05$ vs. control, 1-way ANOVA.

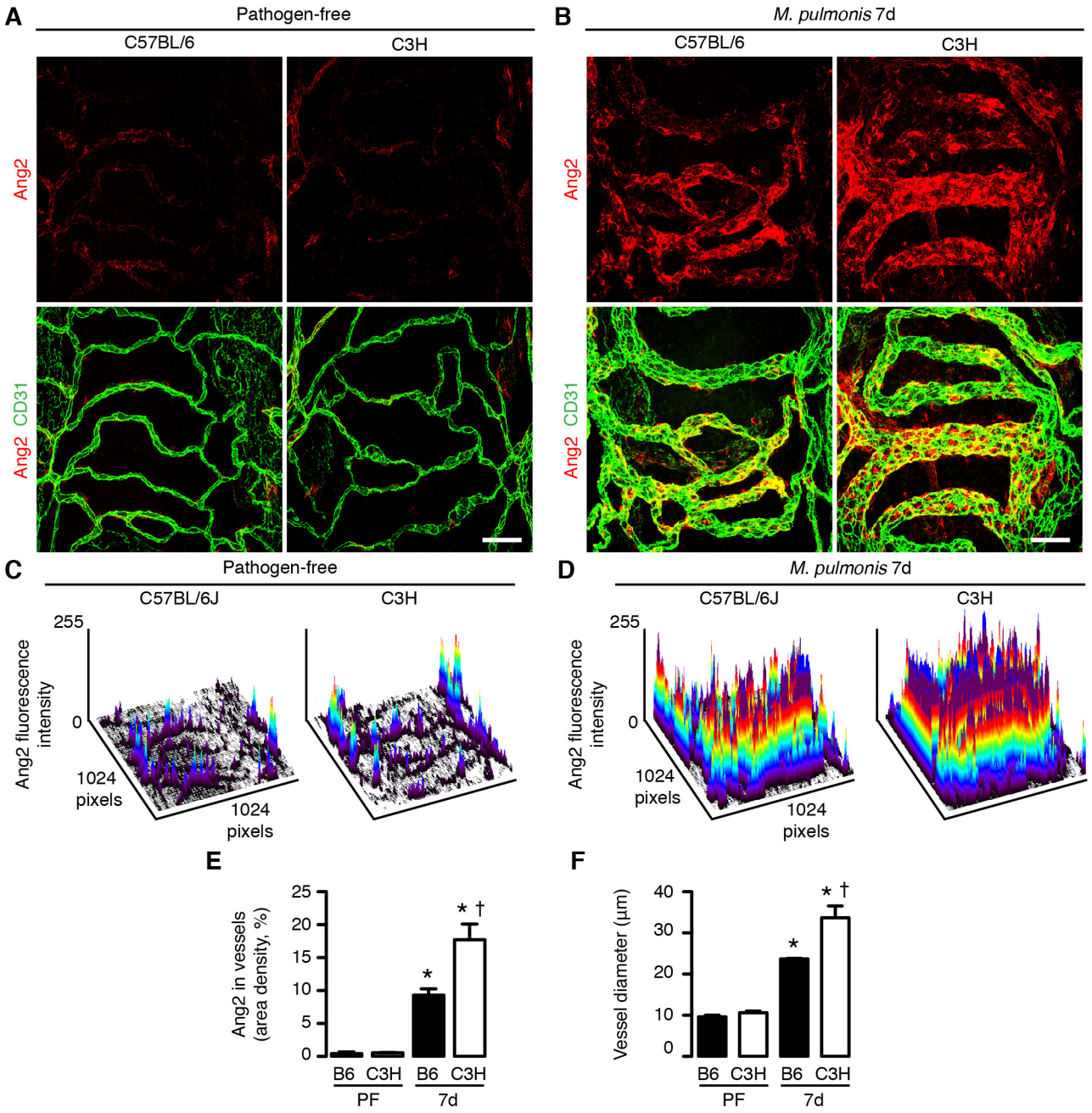

Supplemental Figure 4. Comparison of Ang2 and vascular remodeling after infection in susceptible (C3H) vs. resistant (C57BL/6) mouse strains. (**A** and **B**) Weak Ang2 immunofluorescence in tracheal blood vessels of C57BL/6 and C3H mice under pathogen-free conditions (**A**) and stronger Ang2 staining in both strains after *M. pulmonis* infection for 7 days, but Ang2 staining and vascular enlargement are greater in the C3H mouse (**B**), consistent with greater susceptibility of C3H mice to *M. pulmonis* infection (7). Scale bars in A and B, 50 μm. (**C** and **D**) Surface plots of confocal microscopic images showing Ang2 fluorescence intensity, stronger for both strains after infection but highest in the C3H strain. (**E** and **F**) Measurements of Ang2 staining (**E**) and capillary size (**F**) over cartilage rings in C57BL/6 (B6) and C3H mice without (PF) or with infection (7d) (n = 6 per group). **P* < 0.05 vs. corresponding pathogen-free control; †*P* < 0.05 vs. corresponding C57BL/6 (B6) mice, 1-way ANOVA.

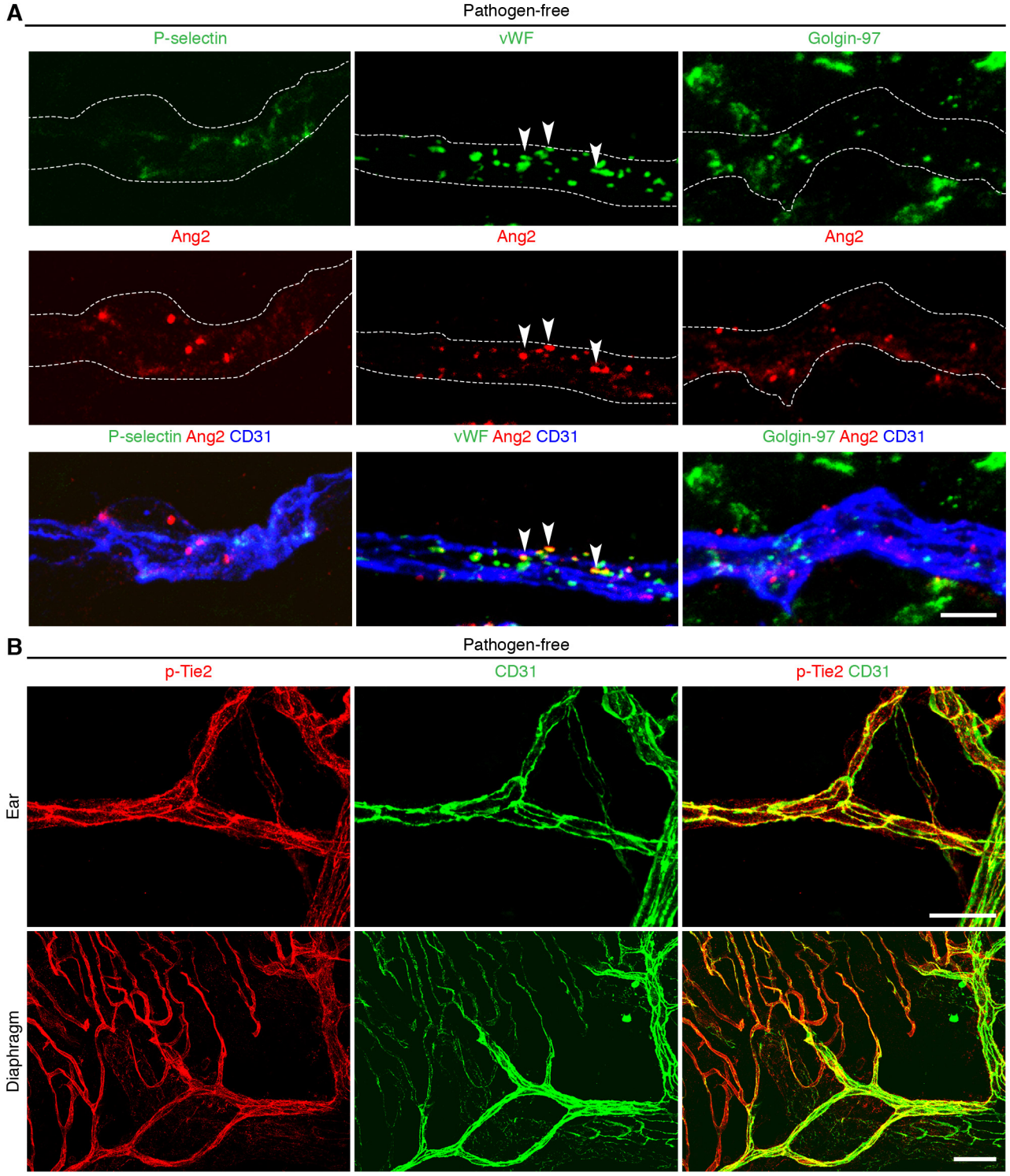

Supplemental Figure 5. Ang2 colocalization with vWF in endothelial cells and p-Tie2 in blood vessels under baseline conditions. (**A**) Strong colocalization of Ang2 with vWF, but not with P-selectin or Golgin-97 in tracheal blood vessels of pathogen-free mice. Arrowheads indicate colocalization of Ang2 and vWF. Scale bar, 10 μm. (**B**) Strong p-Tie2 immunoreactivity in blood vessels of ear skin (top) and diaphragm (bottom) under baseline conditions. Scale bars, 20 μm for ear skin and 50 μm for diaphragm.

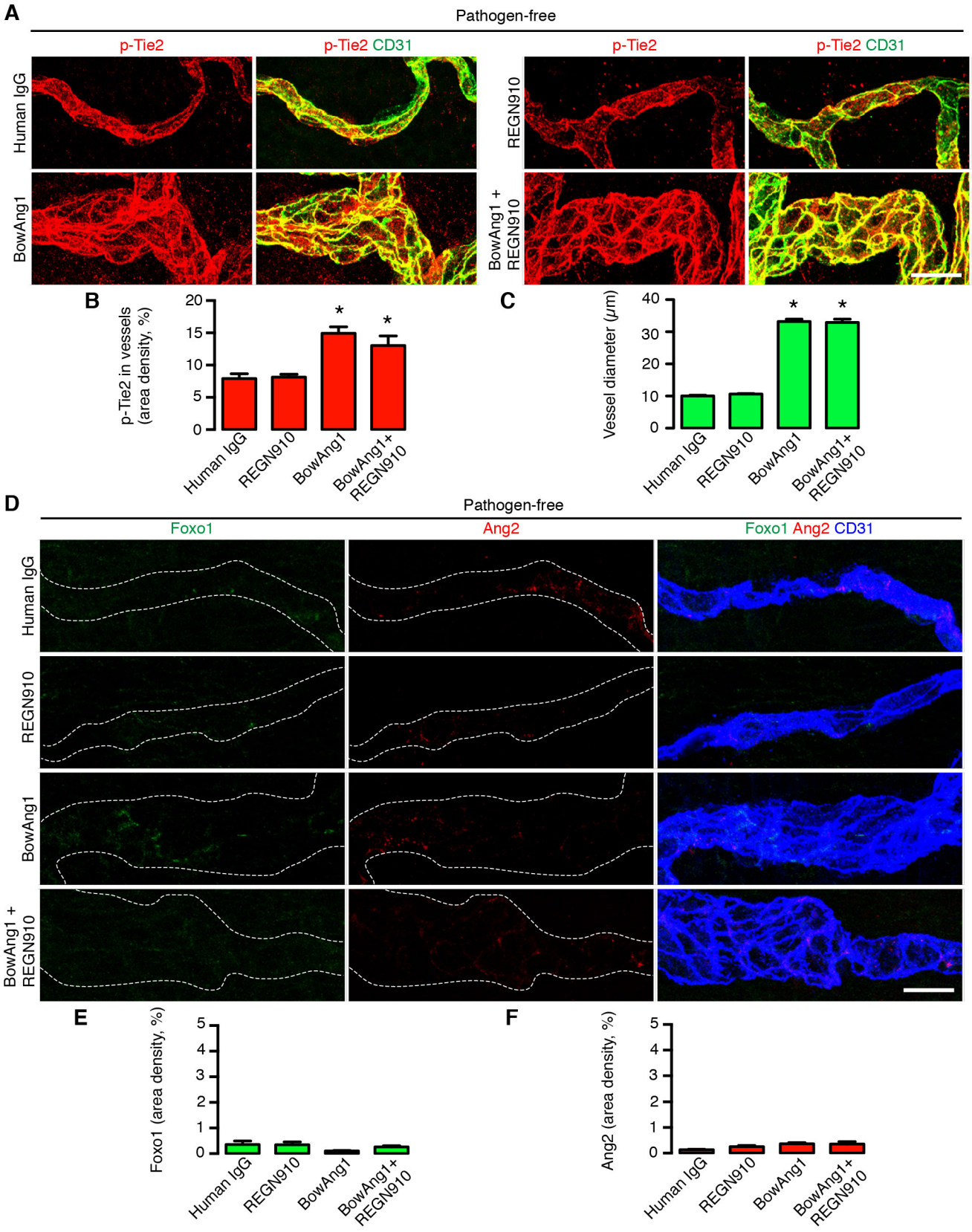

Supplemental Figure 6. Effects of angiopoietins on p-Tie2, Foxo1, and vascular remodeling under baseline conditions. (**A**) Moderate to strong p-Tie2 in tracheal blood vessels of pathogen-free mice treated for 7 days with control antibody (human IgG), anti-Ang2 (REGN910), BowAng1, or BowAng1 plus REGN910. Treatment with BowAng1 alone or with REGN910 is accompanied by stronger p-Tie2 and vascular enlargement. (**B** and **C**) Measurements of p-Tie2 staining (**B**) and capillary size (**C**) in groups shown in A (n = 8-10 per group). *$P < 0.05$ vs. IgG control, by 1-way ANOVA. (**D**) Little or no nuclear Foxo1 or Ang2 staining in blood vessels in the same groups shown in A, which had high p-Tie2. Scale bars in A and D, 25 μm. (**E** and **F**) Measurements of nuclear Foxo1 (**E**) and Ang2 staining (**F**) in groups shown in D (n = 8 per group). No differences from IgG control, 1-way ANOVA.

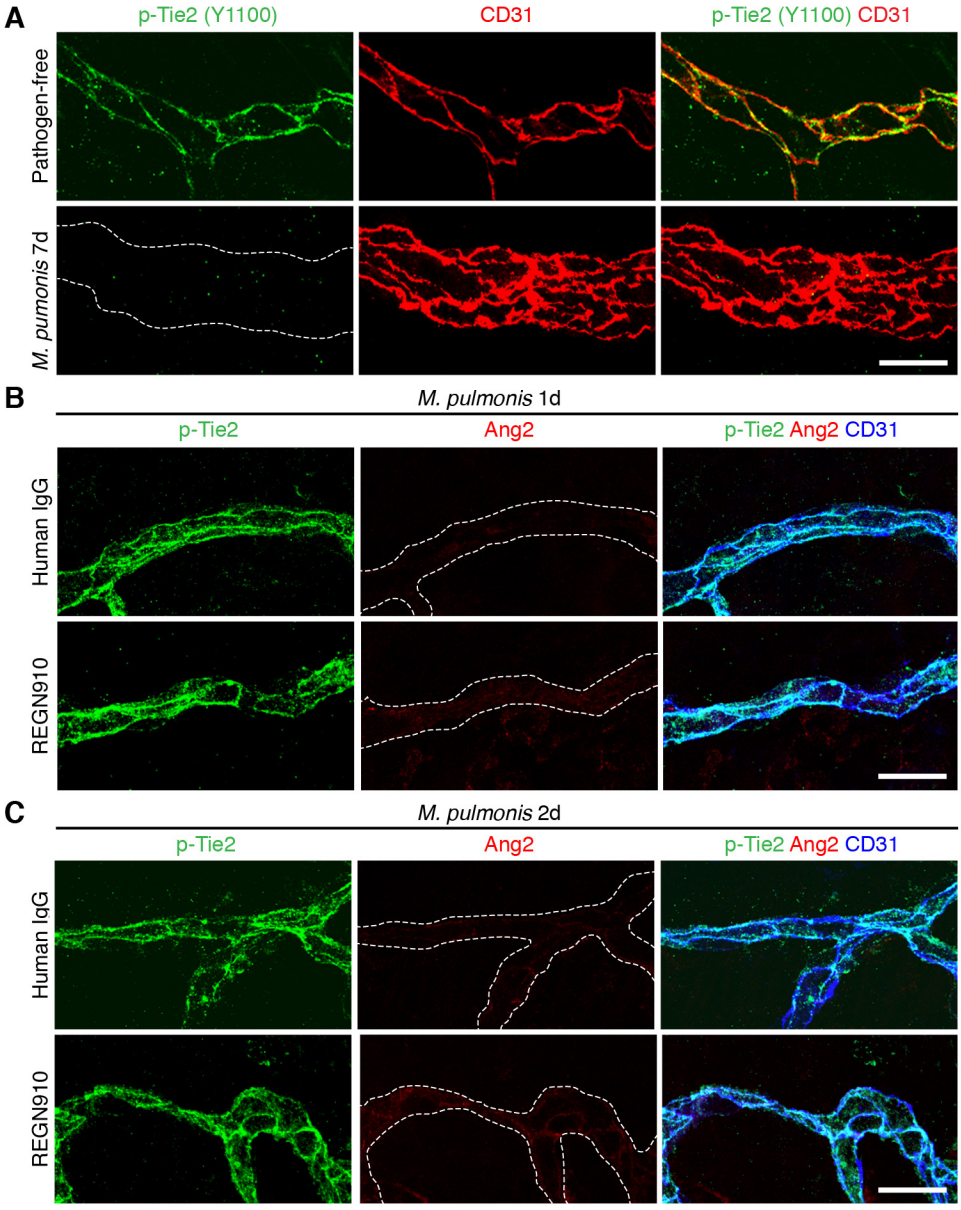

Supplemental Figure 7. Comparison of p-Tie2 and Ang2 with or without infection. (**A**) Strong p-Tie2 at Y1100 in blood vessels of pathogen-free mouse compared to weak or absent p-Tie2 in enlarged vessels after *M. pulmonis* infection for 7 days. (**B** and **C**) Similarly weak Ang2 and strong p-Tie2 immunofluorescence in tracheal capillaries of mice infected for 1 day (**B**) or 2 days (**C**) and no evidence of difference between treatment of control antibody (human IgG) or anti-Ang2 (REGN910). Dashed white lines delineate vessel borders marked by CD31. Scale bars, 25 μm.

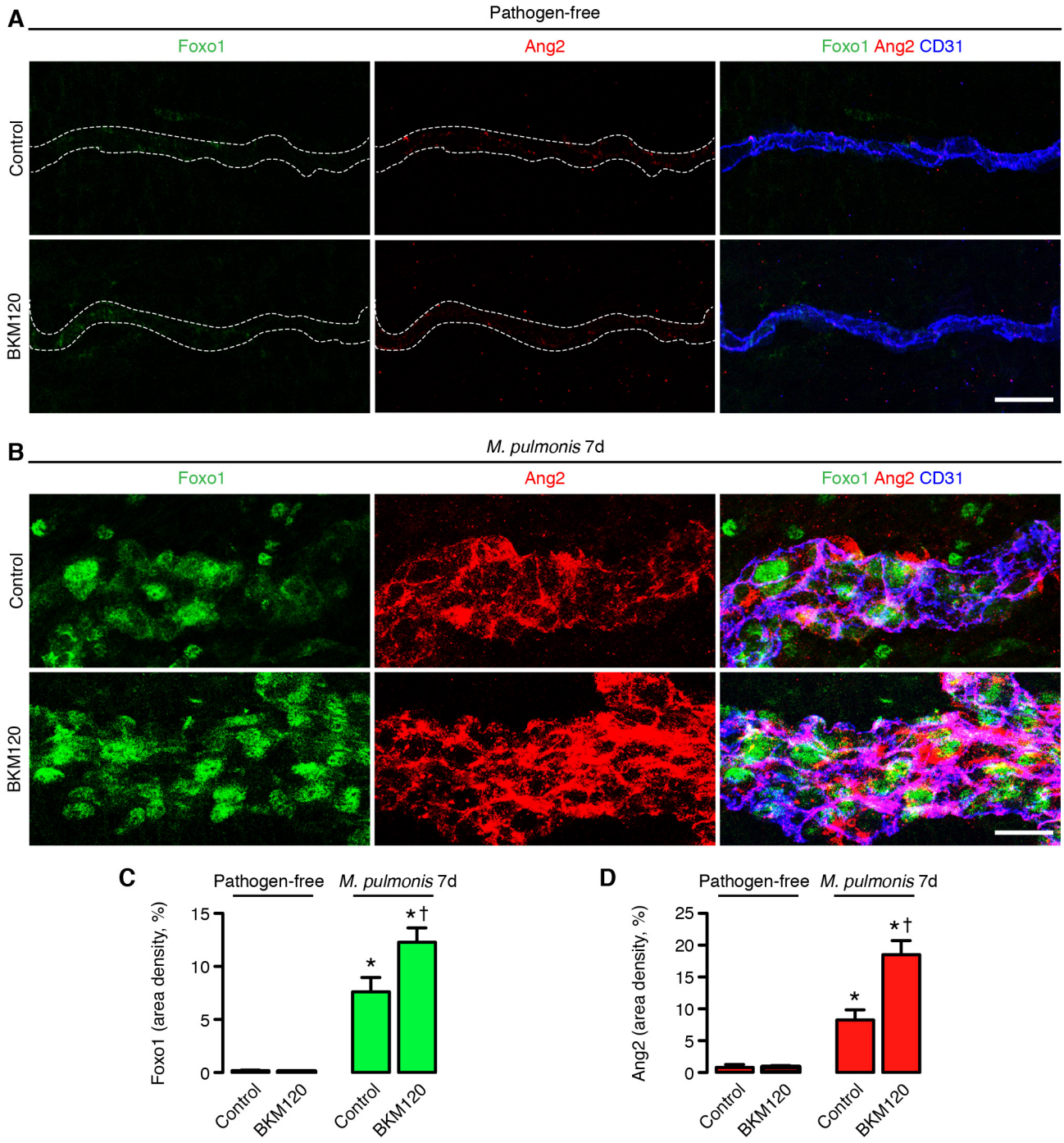

Supplemental Figure 8. Increased Foxo1 activation and Ang2 expression after PI3K/Akt inhibition in infection. (**A**) Weak or absent Foxo1 and Ang2 immunofluorescence in normal vessel of pathogen-free mice after control treatment (PBS) or PI3K/Akt blockade by BKM120. Dashed white lines delineate vessel borders marked by CD31. (**B**) Comparison of blood vessels in control or BKM120 treated mice after *M. pulmonis* infection for 7 days, showing exaggerated nuclear Foxo1 and cytoplasmic Ang2 staining after BKM120. Scale bars in A and B, 20 μm. (**C** and **D**) Measurements of Foxo1 (**C**) and Ang2 (**D**) staining in groups shown in A and B (n = 4 per group). *$P < 0.05$ vs. pathogen-free controls; †$P < 0.05$ vs. infected controls, 1-way ANOVA.

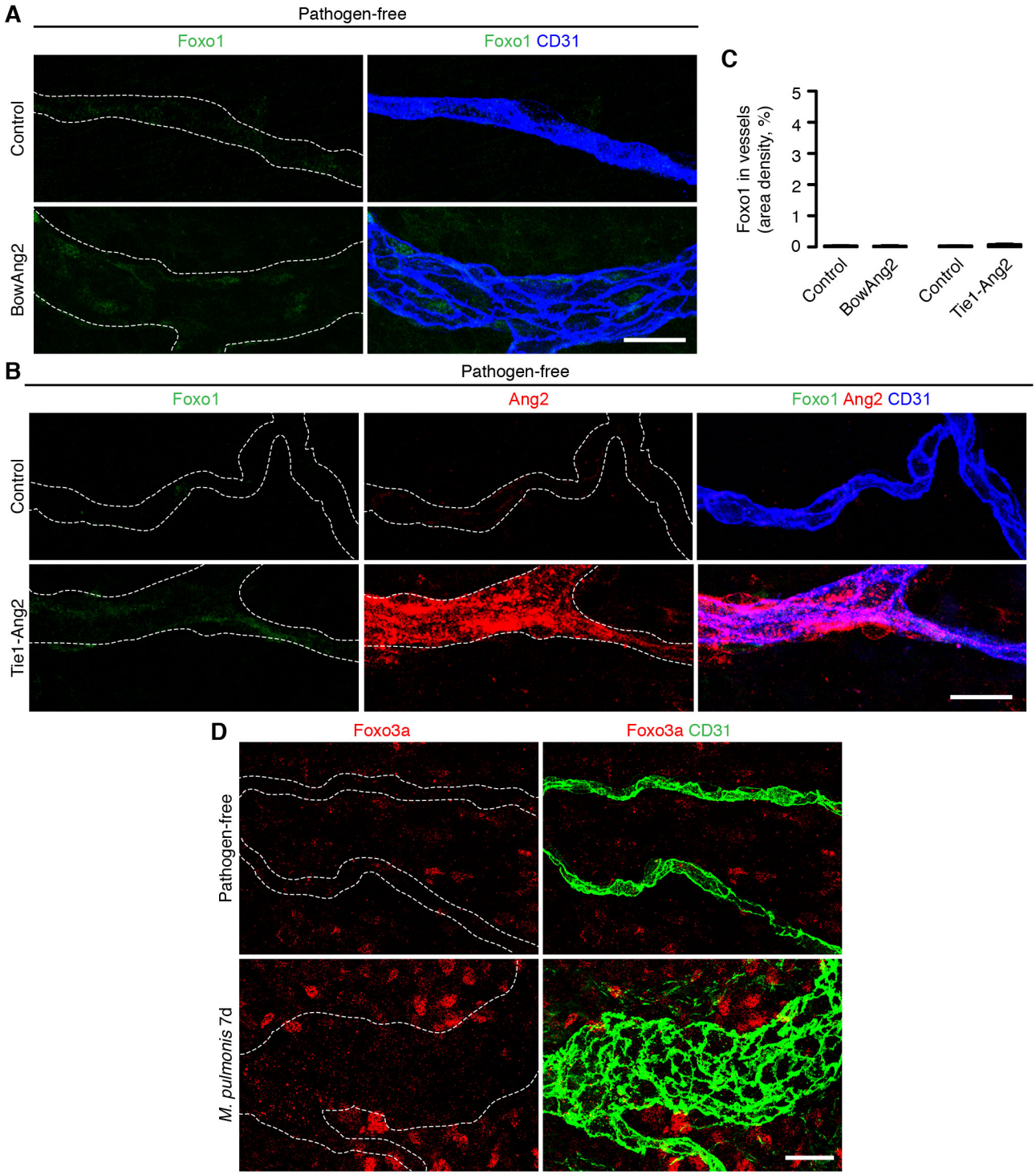

Supplemental Figure 9. Characterization of Foxo regulation in endothelial cells with Ang2 overexpression. (**A**) Nuclear Foxo1 immunofluorescence is similarly weak in a normal tracheal blood vessel and in an enlarged vessel after BowAng2 given to a pathogen-free mouse for 7 days. (**B**) Nuclear Foxo1 is weak or absent in enlarged blood vessel of a pathogen-free Tie1-Ang2 mouse aged 8 weeks, whereas Ang2 staining is strong in this vessel compared to wild-type control. (**C**) Measurement of Foxo1 staining in groups shown in A and B (n = 4 per group). Differences were not significant by Student's *t* test. (**D**) Weak Foxo3a immunofluorescence (red) in the trachea of pathogen-free mouse, compared to strong Foxo3a staining after *M. pulmonis* infection for 7 days. Endothelial cells are marked by CD31 staining (green). Little or no Foxo3a colocalizes with CD31, indicating that most Foxo3a staining is not in endothelial cells. Scale bars in A, B, and D, 25 μm.

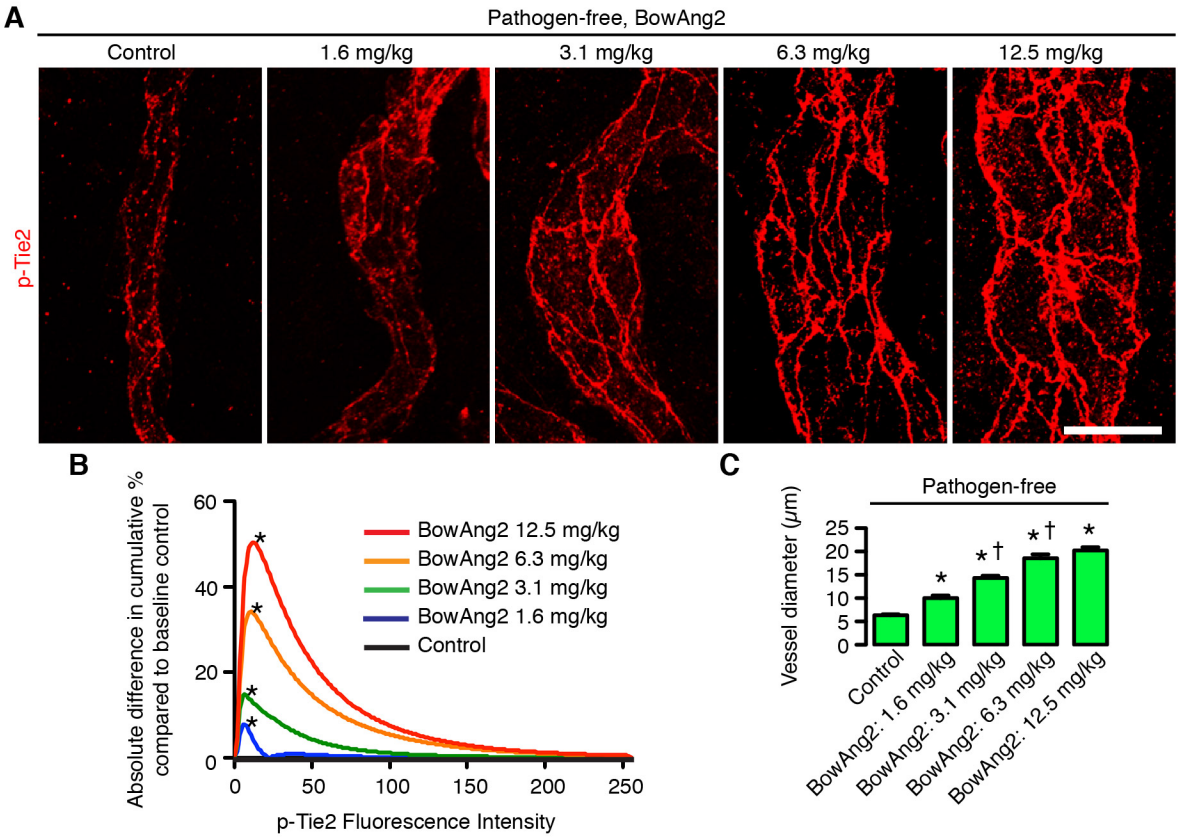

Supplemental Figure 10. Effects of Ang2 overexpression on p-Tie2 and vascular enlargement under baseline conditions.
(**A**) Increasing p-Tie2 and vessel size with increasing BowAng2 dose given to pathogen-free mice for 7 days. Scale bar, 20 μm.
(**B**) Comparison of the absolute difference from baseline control in cumulative percentage of pixels at each fluorescence intensity for the indicated dose of BowAng2 given for 7 days (n = 4 per group). **P* < 0.05 vs. control, Kolmogorov-Smirnov 2-Sample Test on cumulative pixel percentage data. (**C**) Measurement of vessel size in groups shown in A (n = 4-5 per group). **P* < 0.05 vs. untreated control; †*P* < 0.05 vs. next lower BowAng2 dose, 1-way ANOVA.

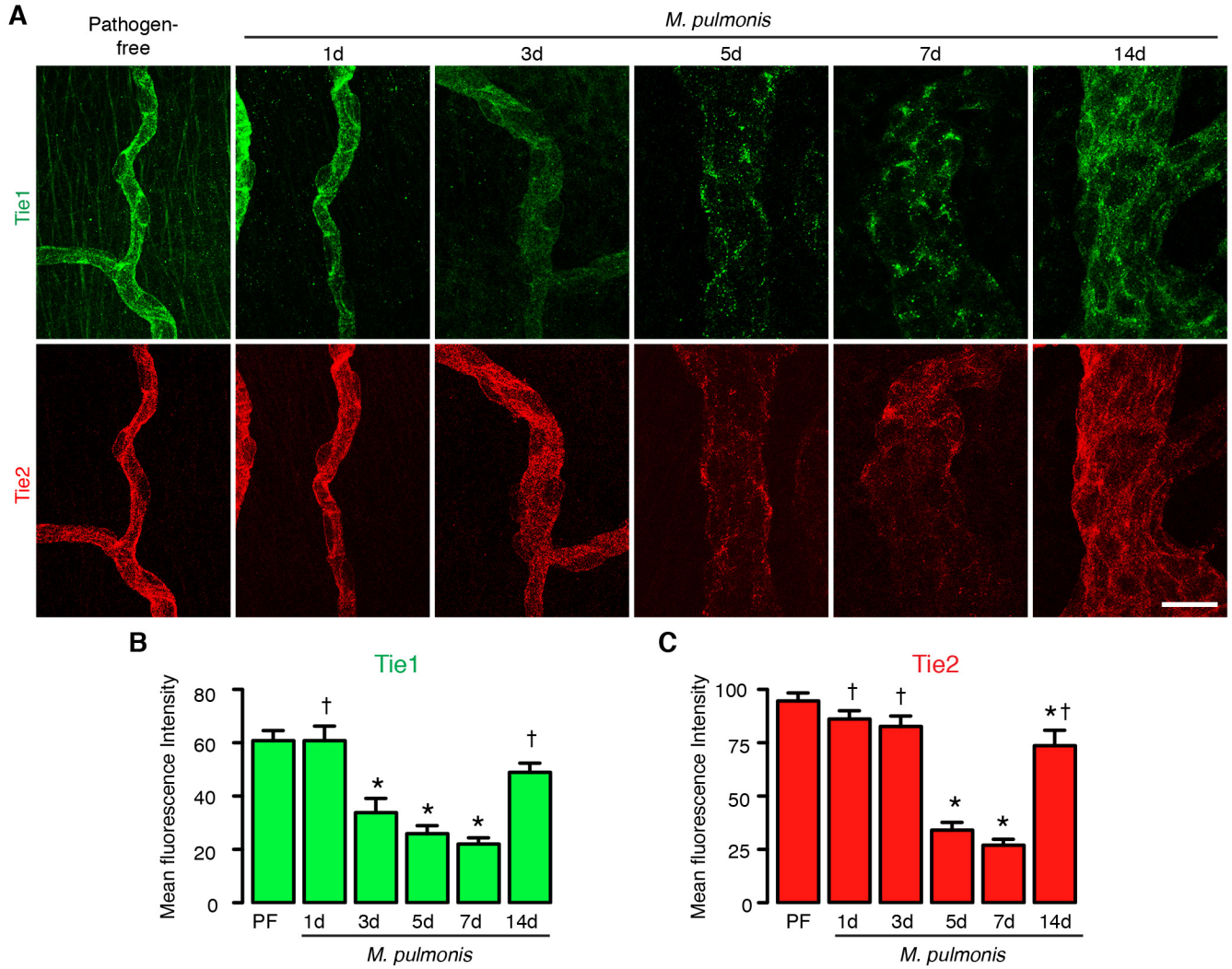

Supplemental Figure 11. Duration dependent changes in Tie1 and Tie2 after *M. pulmonis* infection. (**A**) Progressive reduction in Tie1 and Tie2 immunoreactivities in tracheal capillaries over cartilage rings after *M. pulmonis* infection for 1, 3, 5 or 7 days (d) and partial recovery at day 14 of infection. The distribution of Tie1 in endothelial cells at 5 and 7 days is consistent with localization in the Golgi apparatus. Tie1 and Tie2 at 14 days are stronger than at 7 days. Scale bar, 20 μm. (**B** and **C**) Measurements of Tie1 (**B**) and Tie2 (**C**) mean fluorescence intensity for groups shown in A (n = 5-9 per group). **P* < 0.05 vs. pathogen-free control; †*P* < 0.05 vs. infection for 7 days, 1-way ANOVA.

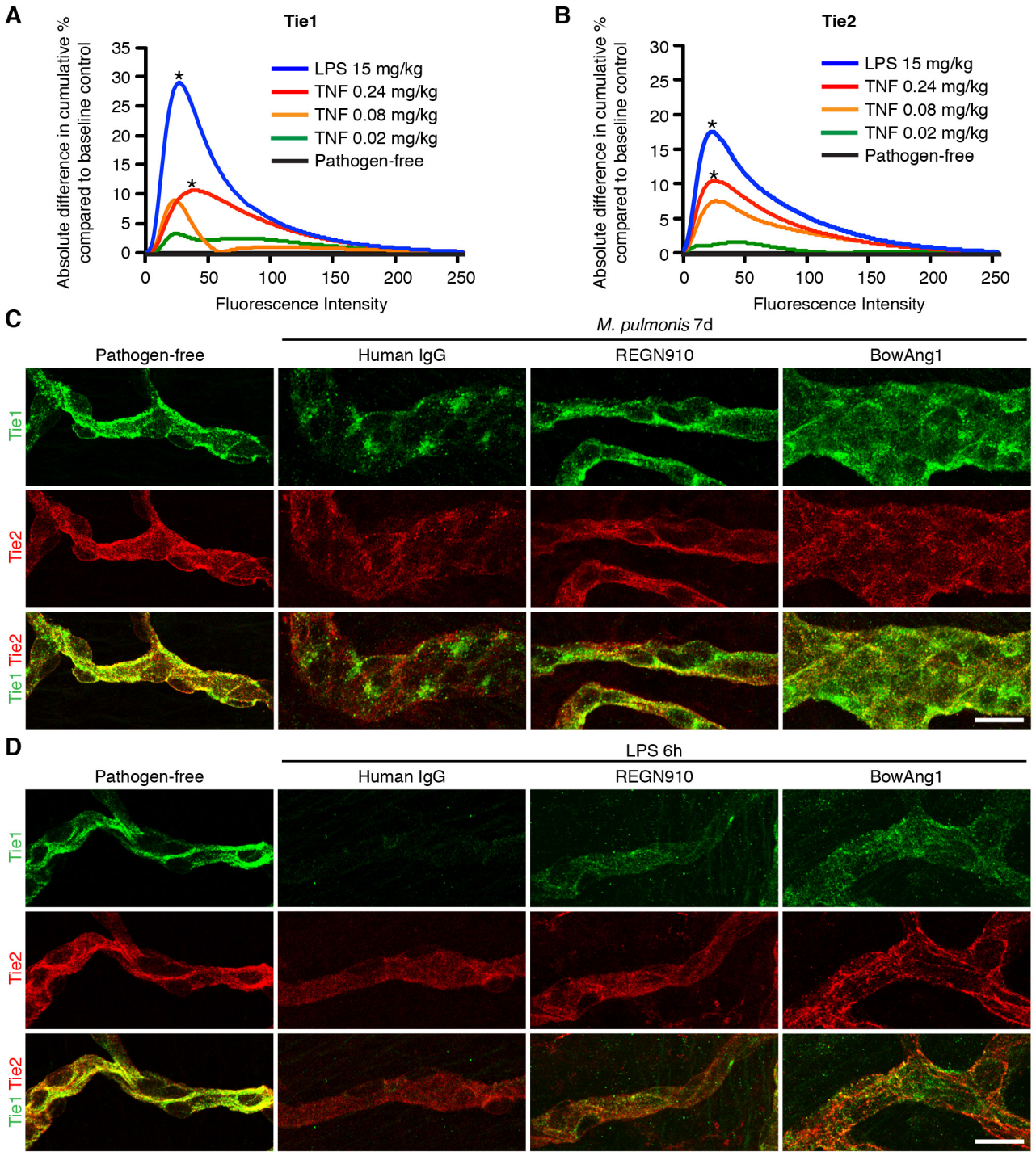

Supplemental Figure 12. Prevention of Tie1 and Tie2 reduction after *M. pulmonis* infection, LPS, or TNF-α by Ang2 inhibitor or Tie2 agonist. (**A** and **B**) Comparison of effects of LPS (15 mg/kg ip) and dose-response effects of TNF-α (0.02 – 0.24 mg/kg iv) for 6 hours on intensity of Tie1 and Tie2 immunoreactivities in tracheal blood vessels. Curves show absolute difference between each experimental group and pathogen-free controls (x-axis) for the cumulative percentage of pixels at each fluorescence intensity for Tie1 (**A**) and Tie2 (**B**) (n = 4 per group). **P* < 0.05 vs. pathogen-free controls, Kolmogorov-Smirnov 2-Sample Test. (**C**) Strong Tie1 and Tie2 in control vessels (pathogen-free) compared to weak staining after *M. pulmonis* infection for 7 days accompanied by control human IgG. After infection, Tie1 has a patchy distribution in endothelial cell cytoplasm, consistent with localization in the Golgi apparatus. The reduction in Tie1 and Tie2 was less when infection was accompanied by anti-Ang2 antibody REGN910 or Tie2-agonist BowAng1. The latter also exaggerated vessel enlargement. (**D**) Similar changes in Tie1 and Tie2 were found after LPS for 6 hours (15 mg/kg ip), where Tie1 was nearly absent and Tie2 was weak, compared to strong staining in pathogen-free controls. The reductions in Tie1 and Tie2 were less when LPS was preceded by REGN910 or BowAng1. Scale bars in C and D, 20 μm.

Supplemental References

1. Daly, C., Eichten, A., Castanaro, C., Pasnikowski, E., Adler, A., Lalani, A.S., Papadopoulos, N., Kyle, A.H., Minchinton, A.I., Yancopoulos, G.D., et al. Angiopoietin-2 functions as a Tie2 agonist in tumor models, where it limits the effects of VEGF inhibition. *Cancer Res*. 2013; 73 (1): 108-118.
2. Fiedler, U., Reiss, Y., Scharpfenecker, M., Grunow, V., Koidl, S., Thurston, G., Gale, N.W., Witzenrath, M., Rosseau, S., Suttorp, N., et al. Angiopoietin-2 sensitizes endothelial cells to TNF-alpha and has a crucial role in the induction of inflammation. *Nat Med*. 2006; 12 (2): 235-239.
3. Maisonpierre, P.C., Suri, C., Jones, P.F., Bartunkova, S., Wiegand, S.J., Radziejewski, C., Compton, D., McClain, J., Aldrich, T.H., Papadopoulos, N., et al. Angiopoietin-2, a natural antagonist for Tie2 that disrupts in vivo angiogenesis. *Science*. 1997; 277 (5322): 55-60.
4. Fiedler, U., Scharpfenecker, M., Koidl, S., Hegen, A., Grunow, V., Schmidt, J.M., Kriz, W., Thurston, G., and Augustin, H.G. The Tie-2 ligand angiopoietin-2 is stored in and rapidly released upon stimulation from endothelial cell Weibel-Palade bodies. *Blood*. 2004; 103 (11): 4150-4156.
5. Korhonen, E., Lampinen, A., Giri, H., Anisimov, A., Kim, M., Allen, B., Fang, S., D'Amico, G., T., S., Lohela, M., et al. Tie1 controls angiopoietin function in vascular remodeling and inflammation. *J Clin Invest*. 2016.
6. Wagner, D.D., and Frenette, P.S. The vessel wall and its interactions. *Blood*. 2008; 111 (11): 5271-5281.
7. Gong, S., Zheng, C., Doughty, M.L., Losos, K., Didkovsky, N., Schambra, U.B., Nowak, N.J., Joyner, A., Leblanc, G., Hatten, M.E., et al. A gene expression atlas of the central nervous system based on bacterial artificial chromosomes. *Nature*. 2003; 425 (6961): 917-925.
8. Cartner, S.C., Simecka, J.W., Lindsey, J.R., Cassell, G.H., and Davis, J.K. Chronic respiratory mycoplasmosis in C3H/HeN and C57BL/6N mice: lesion severity and antibody response. *Infect Immun*. 1995; 63 (10): 4138-4142.